Structures and Magnetic Properties of Novel 1-D Coordination Polymers Containing Both Dicyanamide and Pyridine-Type Ligands

Jamie L. Manson,* Atta M. Arif,* Christopher D. Incarvito,† Louise M. Liable-Sands,†
Arnold L. Rheingold,† and Joel S. Miller*

*Department of Chemistry, University of Utah, 315 S. 1400 E. RM Dock, Salt Lake City, Utah 84112-0850; and
†Department of Chemistry, University of Delaware, Newark, Delaware 19716

DEDICATED TO PETER DAY ON THE OCCASION OF HIS 60TH BIRTHDAY

Three novel 1-D coordination polymers consisting of $\{Mn[N(CN)_2]_2\}_\infty$ structural units and $L = 2$ pyridines (i.e., **2**), 2,2′-bipyridine (i.e., **3**), and 4,4′-bipyridine (i.e., **4**) have been synthesized and characterized by single crystal X-ray crystallography and magnetic susceptibility studies. Compound **2** crystallizes in the monoclinic space group $P2_1/n$ with $a = 7.5401\,(7)$ Å, $b = 13.2643\,(4)$ Å, $c = 8.6973\,(9)$ Å, $\beta = 114.954\,(2)°$, $V = 788.65\,(11)$ Å^3, and $Z = 2$ with $R(R_w) = 0.0451\,(0.1067)$. In **2**, linear 1-D chains containing *trans-μ*-$[N(CN)_2]^-$ ligands and two pyridine ligands are formed while *cis-μ*-$[N(CN)_2]^-$ coordination gives rise to zigzag chains with chelated 2,2′-bipyridine ligands in **3** which crystallizes in the monoclinic space group $C2/c$ with $a = 6.6769\,(3)$ Å, $b = 17.2008\,(2)$ Å, $c = 13.0142\,(4)$ Å, $b = 90.110\,(4)°$, $V = 1494.65\,(8)$ Å^3, and $Z = 4$ with $R(R_w) = 0.0514\,(0.1218)$. Interestingly, incorporation of 4,4′-bipyridine into the structure of **4** produces a unique cylindrical 1-D chain consisting of four *trans-μ*-$[N(CN)_2]^-$'s, one coordinated water, and an unusual monodentate 4,4′-bipyridine ligand. X-ray crystallography established the orthorhombic space group $Iba2$ with $a = 22.378\,(6)$ Å, $b = 22.517\,(5)$ Å, $c = 13.519\,(5)$ Å, $V = 6812\,(3)$ Å^3, and $Z = 8$ with $R(R_w) = 0.0384\,(0.0861)$. The magnetic susceptibilities of each compound were studied in the 2–300 K temperature range and the data fitted to the 1-D Fisher chain model for $S = 5/2$ with g-values of 2.00 and intrachain exchange constants, $J/k_B = -0.10, -0.17$, and -0.24 K for **2**, **3**, and **4**, respectively. © 1999 Academic Press

INTRODUCTION

Coordination polymers extended in 1, 2, and 3 dimensions have received much attention in the past few years due to their fascinating and potentially useful properties such as catalysis (1), conductivity (including superconductivity) (2), host–guest applications (3), and bulk magnetic behavior (4).

Molecule-based magnets have been at the forefront of interdisciplinary research since the ferromagnetic electron transfer salt $[FeCp_2^*]^{+\cdot}[TCNE]^{-\cdot}$ (Cp*, cyclopentadienide; TCNE, tetracyanoethylene) (4, 5) and the ferrimagnetic $Mn^{II}Cu^{II}$ chains (4, 6) were discovered to magnetically order at low temperatures (6, 7). Typically, molecule-based magnetic materials are prepared using organic/organometallic methodologies under mild conditions, an advantage over conventional metallurgical processes. In this manner, the first polymeric molecule-based magnet with a T_c exceeding room temperature, $V(TCNE)_2 \cdot yCH_2Cl_2$, was prepared and magnetically characterized (7). Recently, other examples in the $M(TCNE)_2$ ($M = Mn$, Fe, Co, and Ni) series have been described, however, their structures remain elusive (8).

Conjugated ligands capable of superexchange (e.g., cyano, oxalato, etc.) between paramagnetic metal centers have been shown to display exceptional cooperative phenomena (4, 6, 9, 10). Composed solely of paramagnetic metal centers and diamagnetic bridging ligands, $V[Cr(CN)_6]_{0.86}$ is the second example discovered to magnetically order above room temperature (9a). Polydentate ligands containing nitrile substituents are generally good Lewis bases capable of coordination to acidic transition metal centers, thus creating interesting structural motifs (11).

Dicyanamide, $[N(CN)_2]^-$, was selected due to its coordination versatility ranging from being monodentate to μ_4-coordination as reported for $(CH_3)_2Tl[N(CN)_2]$, **1a** (12) (Scheme 1). Examples of monodentate $[N(CN)_2]^-$, **1b**, where coordination occurs via a terminal N have been reported for $[Cu(phen)_2\{N(CN)_2\}][C(CN)_3]$ (13) and $[Cu(phen)_2\{N(CN)_2\}_2]$ (14). A few examples of bidentate $[N(CN)_2]^-$, **1c**, have been reported such as $Ag[N(CN)_2]$ (15) and $(CH_3)_2Sn[N(CN)_2]$ (16), which form 1-D zigzag chains, while $Zn[N(CN)_2]_2$ (17) consists of 2-D buckled sheets. Three-coordinate $[N(CN)_2]^-$, **1d**, is observed in the
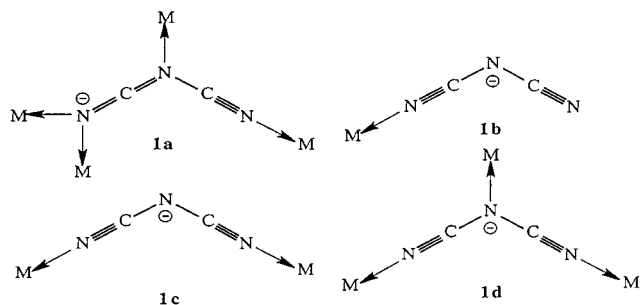
SCHEME 1

ferromagnetic rutile-like material α-Co[N(CN)$_2$]$_2$ (18). In order to evaluate the magnetic interaction between metal sites separated by large distances, high-spin ($S = 5/2$) Mn^{II} was utilized because of its large magnetic moment due to the five unpaired electrons, minimal magneto-crystalline anisotropy, and good Lewis acidity. Additional ligands such as coordinating amines (Lewis bases) in combination with dicyanamide are expected to produce novel structure types. Herein, we report the synthesis, crystal structures, and magnetic properties of Mn[N(CN)$_2$]$_2$(py)$_2$ (py, pyridine), **2**, Mn[N(CN)$_2$]$_2$(2,2'-bipy) (bipy, bipyridine), **3**, and Mn[N(CN)$_2$]$_2$(4,4'-bipy) · 3/2H$_2$O, **4**.

EXPERIMENTAL

Physical Measurements

The infrared spectra were recorded on a Bio-Rad FTS-40 Fourier transform spectrometer in the range 4000–600 cm^{-1} as Nujol mulls sandwiched between NaCl plates. Thermal analysis was performed using a TA model 2050 differential scanning calorimeter and TA model 2910 thermogravimetric analyzer in the temperature range 25–500°C. DC magnetization measurements in the 2–300 K range are as previously described (18a). Samples (~ 20 mg) for magnetic measurements were loaded into gelatin capsules and mounted in a plastic straw prior to magnetic measurements. All samples were corrected for core diamagnetism which were 162, 169, and 208×10^{-6} emu/mol for **2**, **3**, and **4**, respectively, as calculated from Pascal's constants.

Mn[N(CN)$_2$]$_2$(py)$_2$, 2

A 5-ml methanol solution of Mn^{II}(py)$_4$(NCS)$_2$ (19) (0.394 mmol, 0.1919 mg) was slowly added to a 5-ml aqueous solution of Na[N(CN)$_2$] (Aldrich) (1.12 mmol, 0.0998 mg) to afford a pale yellow solution. Crystals suitable for X-ray structure determination were obtained in quantitative yield by slow solvent evaporation over a three-

day period. ν_{CN} (Nujol): 2359 w, 2295 s, 2234 s, and 2167 s cm^{-1}. Thermogravimetric analysis shows a sharp weight loss of 45.5% at about 165°C, consistent with the loss of 2 equivalents of coordinated pyridine (45.8% calc.). Anal. calcd. for C$_{14}$H$_{10}$N$_8$Mn: C, 48.74; H, 2.92; N, 32.48. Found: C, 48.61; H, 2.93; N, 32.37.

Mn[N(CN)$_2$]$_2$(2,2'-bipy), 3

A 5-ml aqueous solution of MnCl$_2$ · 4H$_2$O (Fisher Scientific) (1.36 mmol, 0.2686 g) was added slowly to a stirring 15-ml H$_2$O/EtOH solvent mixture containing Na[N(CN)$_2$] (2.71 mmol, 0.2413 g) and 2,2'-bipyridine (Aldrich) (1.35 mmol, 0.2115 g). A yellow microcrystalline powder precipitated immediately and was collected via vacuum filtration and dried *in vacuo* over P$_2$O$_5$ (0.4187 g, 89%). Single crystals were obtained by slow solvent evaporation of the filtrate over a 2-week period. ν_{CN} (Nujol): 2414 w, 2304 m, 2232 m, 2205 s, and 2169 s cm^{-1}. Anal. calcd. for C$_{14}$H$_8$N$_8$Mn: C, 48.99; H, 2.34; N, 32.65. Found: C, 48.90; H, 2.31; N, 32.73.

Mn[N(CN)$_2$]$_2$(4,4'-bipy) · 3/2H$_2$O, 4

A 5-ml aqueous solution of MnCl$_2$ · 4H$_2$O (1.42 mmol, 0.2818 g) was added slowly to a stirring 10-ml H$_2$O/(CH$_3$)$_2$CO solvent mixture containing Na[N(CN)$_2$] (2.87 mmol, 0.2558 g) and 4,4'-bipyridine (Aldrich) (1.43 mmol, 0.2226 g). A pale peach microcrystalline powder precipitated immediately and was collected via vacuum filtration and dried *in vacuo* over P$_2$O$_5$ (0.4577 g, 94%). Long colorless prisms were grown by slow evaporation of the filtrate over a 5-day period. ν_{CN} (Nujol): 2415 w, 2303 m, 2242 m, and 2178 s cm^{-1}. Anal. calcd. for C$_{28}$H$_{22}$N$_{16}$O$_3$Mn$_2$: C, 45.42; H, 2.99; N, 30.27. Found: C, 45.40; H, 2.98; N, 30.18.

STRUCTURE DETERMINATIONS

Mn[N(CN)$_2$]$_2$(py)$_2$, 2

Crystal, data collection, and refinement parameters are given in Table 1. The systematic absences in the diffraction data are uniquely consistent for the reported space group. The structure was solved using direct methods, completed by subsequent difference Fourier syntheses, and refined by full-matrix least-squares procedures. Semi-empirical absorption corrections were not required because there was less than 10% variation in the integrated ψ-scan intensity data. The extended molecule resides periodically on an inversion center. All nonhydrogen atoms were refined with anisotropic displacement coefficients and hydrogen atoms were treated as idealized contributions. All software and sources of the scattering factors are contained in the SHELXTL (5.0) program library (20).

TABLE 1
Summary of Single Crystal X-ray Diffraction Data for Mn[N(CN)$_2$]$_2$(py)$_2$, 2, Mn[N(CN)$_2$]$_2$(2,2′-bipy), 3, and Mn[N(CN)$_2$]$_2$(4,4′-bipy)·3/2H$_2$O, 4

Compound:	Mn[N(CN)$_2$]$_2$(py)$_2$	Mn[N(CN)$_2$]$_2$(2,2′-bipy)$_2$	Mn[N(CN)$_2$]$_2$(4,4′-bipy)·3/2H$_2$O
Formula weight:	345.24	343.22	370.25
Space group:	$P2_1/n$	$C2/c$	$Iba2$
		Cell dimensions	
a (Å):	7.5401 (7)	6.6769 (3)	22.378 (6)
b (Å):	13.2643 (4)	17.2008 (2)	22.517 (5)
c (Å):	8.6973 (9)	13.0142 (4)	13.519 (5)
β (°):	114.954 (2)	90.110 (2)	90
Volume (Å^3):	788.65 (11)	1494.65 (8)	6812 (3)
Z:	2	4	8
p_{calc} (g cm^{-3}):	1.454	1.525	1.444
		Intensity measurements	
λ (MoKα) (Å):	0.71073	0.71073	0.71073
Scan mode:	$\theta/2\theta$	$\theta/2\theta$	$\theta/2\theta$
max θ (°):	28	26	25
Standard reflections:			3 measured every hour
Reflections collected:	2991	3096	3135
Unique reflections with $|F_0| > 2\sigma|F_0|^2$:	1550	1343	2509
μ (mm^{-1}):	0.848	0.895	0.797
		Structure solution and refinement	
Parameters refined:	106	105	476
Agreement factors:	$R = 0.0451,^a R_w = 0.1067^b$	$R = 0.0514,^a R_w = 0.1218^b$	$R = 0.0384,^a R_w = 0.0861^b$
Weighting scheme:			$w = [\sigma^2(I) + 0.0484(I)^2 + 4.1970(I)]^{-1}$

$^a R = \sum(|F_0| - |F_c|/\sum|F_0|$.
$^b R_w = [\sum w(|F_0| - |F_c|)^2/\sum w|F_0|^2]^{1/2}$.

Mn[N(CN)$_2$]$_2$(2,2′-bipy), 3

Data collection and refinement used methods and procedures similar to those for **2**, except the systematic absences in the diffraction data allowed two space groups, Cc and $C2/c$. The latter centrosymmetric choice was preferred due to the stability of the refinement and chemical reasonableness of the resulting structure. The diffraction data also revealed that monoclinic symmetry was the highest possible, a concern arising from the near to 90° β angle.

Mn[N(CN)$_2$]$_2$(4,4′-bipy)·3/2H$_2$O, 4

Crystal, data collection, and refinement conditions are given in Table 1. Structure solution was achieved using direct methods (SIR97) (21) and refined by full-matrix least-squares procedures (SHELXTL97) (20). Diffraction data initially suggested a pseudo-tetragonal unit cell; however, upon data reduction and subsequent refinement this gave unsatisfactory results. Lowering of the symmetry to orthorhombic yielded two possible space groups consistent with the diffraction data, $Iba2$ and centrosymmetric $Ibam$. The former space group was preferred because it significantly improved R_1 and wR_2. O(1), O(2), O(1)′, and O(2)′ were refined as disordered water molecules with 0.5 occupancy each. The structure was solved using direct methods, completed by subsequent difference Fourier mapping, and refined by full-matrix least-squares procedures. Empirical absorption corrections were applied to all data using the ψ-scan method. All nonhydrogen atoms were refined with anisotropic thermal parameters and hydrogen atoms were treated as idealized contributions.

DISCUSSION

Crystal Structures

*Mn[N(CN)$_2$]$_2$(py)$_2$, **2**.* Compound **2** crystallizes in the monoclinic space group $P2_1/n$ with two molecules per unit cell; see Table 1. Figure 1 shows an ORTEP diagram of the asymmetric unit and atom-labeling scheme of **2**. Four different [N(CN)$_2$]$^-$ ligands and two pyridine molecules coordinate to a single Mn^{II} center, generating tetragonally
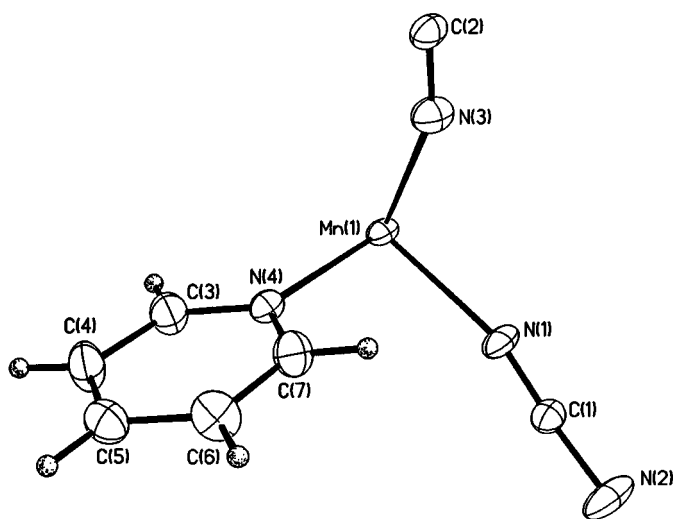
FIG. 1. ORTEP diagram of the asymmetric unit of **2** depicting the atom-labeling scheme.
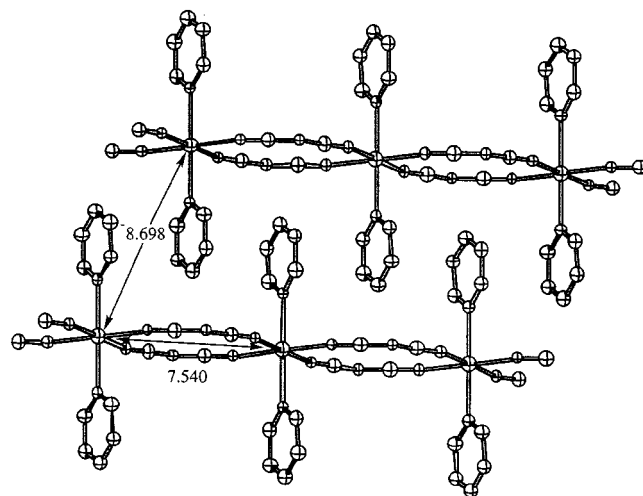

FIG. 2. A segment of two adjacent 1-D chains of **2** displaying the out-of-registry packing arrangement. The shortest intra- and interchain Mn⋯Mn separations (Å) are also shown.

elongated MnN6 octahedra with Mn-N$_{dicyan}$ equatorial distances of 2.227 (2) and 2.234 (3) Å and average 2.231 Å and an axial Mn–N(4) distance of 2.271 (2) Å; see Table 2. Furthermore, the MnN$_6$ octahedron is centered about the

origin and is only slightly distorted with *cis*-N–Mn–N′ angles ranging from 89.02 (9) to 90.98 (9)° and averaging 90.0°. Polymeric 1-D chains are generated parallel to the *a*-axis, with adjacent chains staggered *a*/2 so as to provide

TABLE 2
Selected Bond Lengths (Å) and Bond Angles (°) for Mn[N(CN)$_2$]$_2$(py)$_2$, 2, Mn[N(CN)$_2$]$_2$(2,2′-bipy), 3, and Mn[N(CN)$_2$]$_2$(4,4′-bipy) · 3/2H$_2$O, 4

|					
		Mn[N(CN)$_2$]$_2$(py)$_2$, **2**			
Mn–N(1)	2.227 (2)	Mn–N(4)	2.271 (2)	C(1)–N(2)	1.297 (4)
Mn–N(3)	2.234 (3)	C(1)–N(1)	1.146 (4)	C(3)–N(4)	1.329 (3)
N(1)#1–Mn–N(3)	89.02 (9)	C(1)–N(1)–Mn	162.1 (2)		
N(1)#1–Mn–N(3)#1	90.98 (9)	C(2)–N(3)–Mn	155.6 (2)		
N(1)–Mn–N(4)	89.58 (9)	C(3)–N(4)–Mn	121.1 (2)		
		Mn[N(CN)$_2$]$_2$(2,2′-bipy), **3**			
Mn–N(1)	2.258 (3)	Mn–N(3)	2.230 (4)	C(1)–N(1)	1.342 (4)
Mn–N(2)	2.195 (3)	C(21)–N(2)	1.141 (4)	C(31)–N(4)	1.282 (5)
N(2)–Mn–N(2)#1	102.60 (17)	N(3)–Mn–N(1)#1	94.60 (11)		
N(2)–Mn–N(3)#1	86.50 (13)	N(2)–Mn–N(1)	92.72 (11)		
N(2)#1–Mn–N(3)#1	90.26 (13)	N(2)–Mn–N(1)#1	164.19 (11)		
N(1)#1–Mn–N(1)	72.31 (16)	N(3)#1–Mn–N(3)	174.81 (18)		
		Mn[N(CN)$_2$]$_2$(4,4′-bipy) · 3/2H$_2$O, **4**			
Mn–N(2)	2.187 (6)	Mn–N(8)	2.263 (4)	C(2)–N(2)	1.137 (9)
Mn–N(4)	2.206 (7)	Mn–O(2)	2.220 (11)	C(2)–N(3)	1.280 (12)
N(2)–Mn–N(4)	89.4 (2)	N(7)–Mn–N(8)	85.1 (2)		
N(5)–Mn–N(7)	91.3 (2)	C(6)–N(8)–Mn	121.3 (3)		
N(2)–Mn–O(2)	103.1 (4)	C(4)–N(5)–Mn	167.4 (7)		
N(2)–Mn–N(8)	92.9 (2)	C(2)–N(2)–Mn	170.2 (6)		
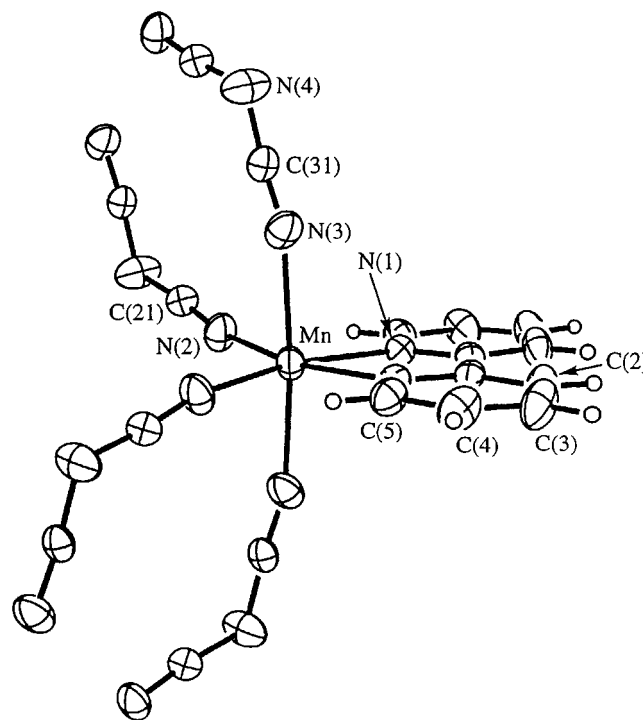
FIG. 3. ORTEP diagram of the asymmetric unit of **3** depicting the atom-labeling scheme. Ellipsoids are shown at the 35% probability.
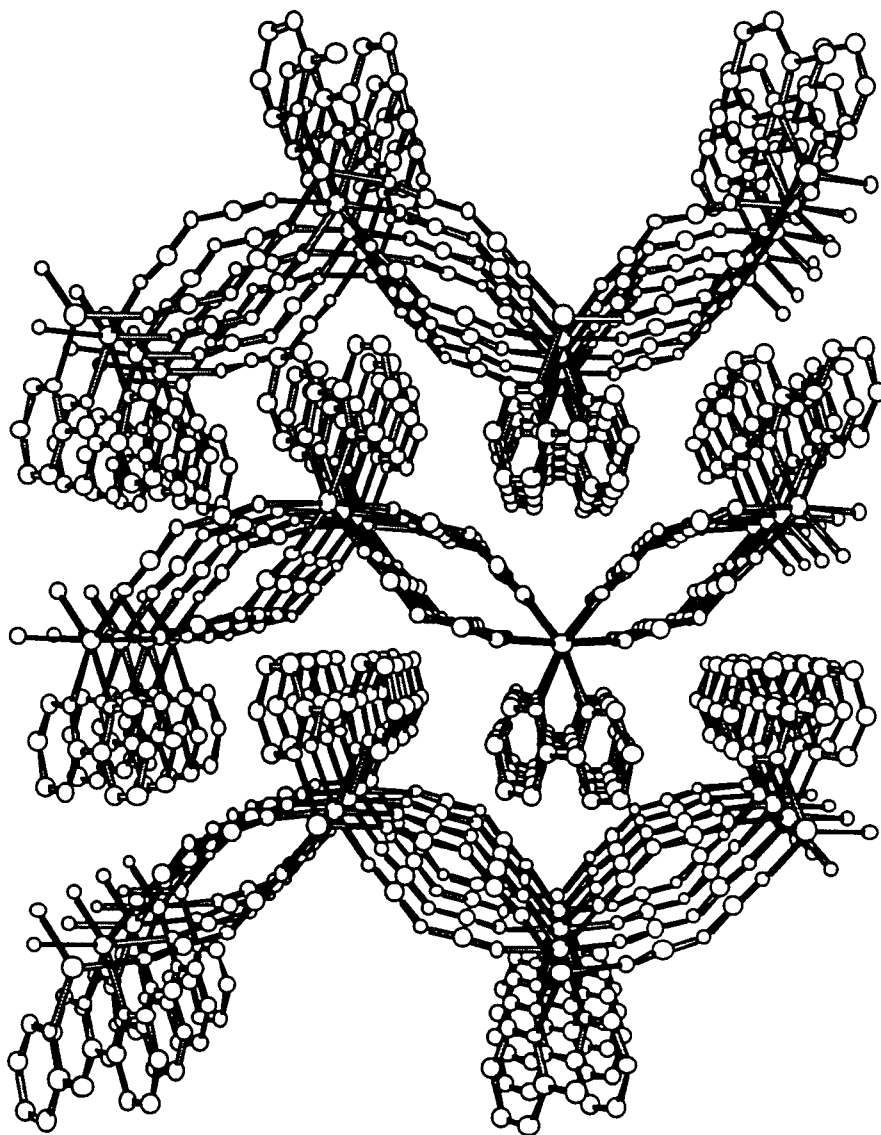
FIG. 4. Crystal packing of the 1-D chains in **3** emphasizing the pseudo-2-D network structure.

a more efficient packing arrangement; see Fig. 2. Weak π–π interactions are evident, with the shortest distance between pyridine planes of adjacent chains being ~ 3.6 Å, thus forming planar 2-D sheets held together by van der Waals forces with the shortest intrachain Mn$\cdots$Mn (7.541 Å) being shorter than the shortest interchain M$\cdots$M' (8.697 Å).

Mn[N(CN)$_2$]$_2$(2,2'-bipy), **3**. Compound **3** forms an extended structure with a zigzag 1-D chain, where Mn^{II} centers are bound to four μ-N≡C–N–C≡N ligands and one chelating 2,2'-bipyridine ligand; see Fig. 3. The Mn^{II} coordination sphere is distorted octahedral with Mn–N distances of 2.258 (3), 2.195 (3), and 2.230 (4) Å. The effect of the

distortion is readily seen in the *cis*-N–Mn–N' bond angles, which vary from 72.31 (16) to 102.60 (17)° for N(1)#1–Mn–N(1) and N(2)–Mn–N(2)#1, respectively. [N(CN)$_2$]$^-$ bridging ligands retain approximate C_{2v} symmetry with C(21)–N(2) and C(31)–N(3) bond distances of 1.141 (4) and 1.131 (4) Å, respectively. In the solid state, adjacent chains pack in registry and form a 2-D structural motif (Fig. 4), although there are no π–π interactions between chains as distances exceed 3.7 Å.

Mn[N(CN)$_2$]$_2$(4,4'-bipy)·3/2H$_2$O, **4**. Compound **4** crystallizes in the noncentrosymmetric orthorhombic space group *Iba*2 with eight molecules per unit cell. Two
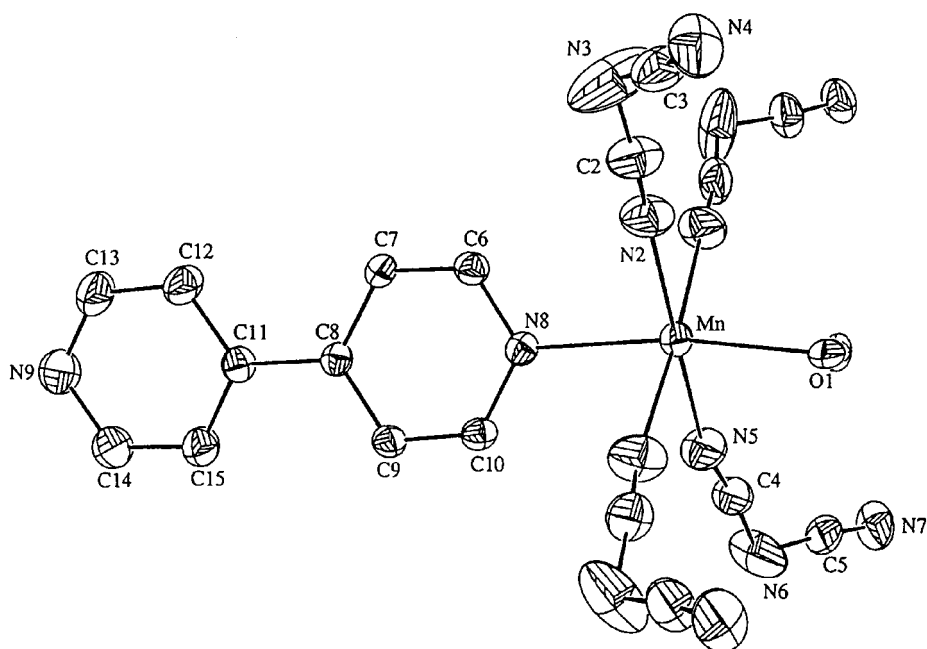
FIG. 5. ORTEP diagram of the local coordination environment of the octahedral Mn center for **4**. Ellipsoids are drawn at the 35% probability.
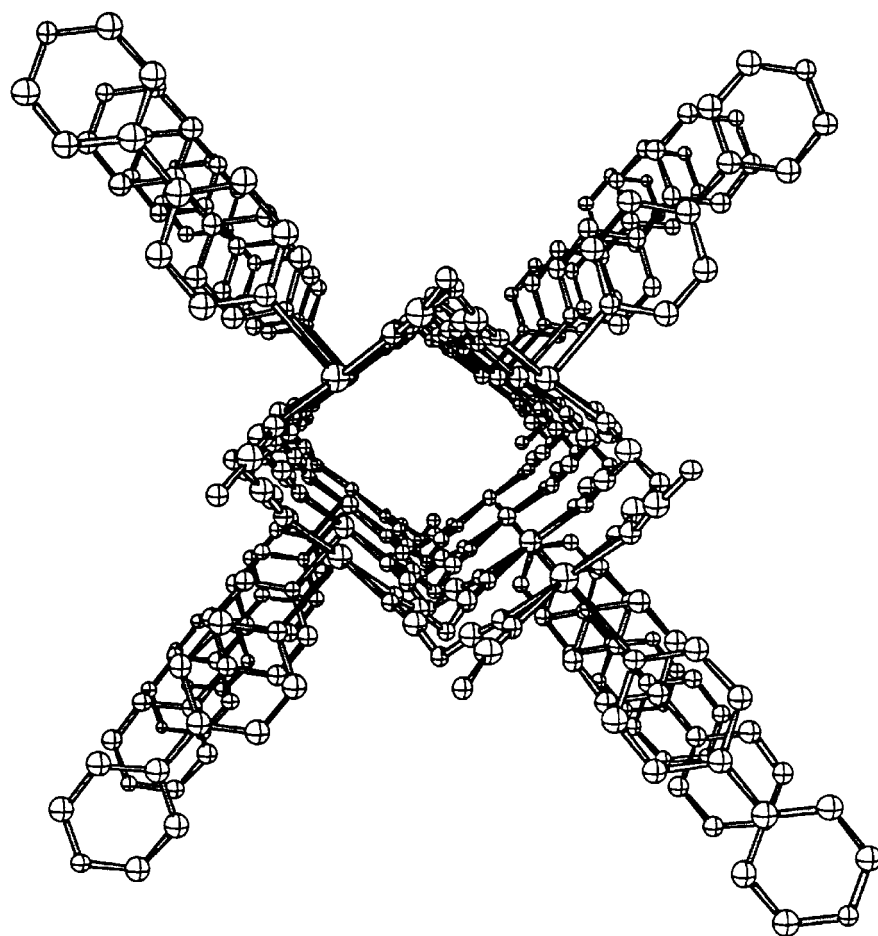

FIG. 6. Perspective view of **4** down the c-axis emphasizing the rhombohedral-type cavities. The H_2O molecules that occupy the cavities have been omitted for clarity.

crystallographically unrelated cylindrical-like 1-D chains are present in the unit cell, but possess nearly identical structural features. The distorted octahedral Mn^{II} coordination sphere consists of four equatorial terminal nitrogens of μ-$[N(CN)_2]^-$, one nitrogen of 4,4'-bypyridine, and one oxygen of water *trans* to one another; see Fig. 5. The four Mn–N(dicyanamide) bond distances range from 2.187 (6) to 2.213 (7) Å and average 2.20 Å, consistent with other Mn^{II}–N distances observed in many materials (22). Due to the bulk size of bipyridine and close proximity of *ortho*-hydrogens to the coordinated metal center, Mn–N(8) is longer at 2.263 (4) Å. Mn–O(1) and Mn–O(2) bond distances are 2.309 (9) and 2.220 (11) Å, respectively, suggesting a weakly bound water molecule. The dicyanamide ligand possesses pseudo-C_{2v} symmetry with $C \equiv N$ bond distances ranging from 1.111 (10) to 1.140 (10) Å. The remaining $[N(CN)_2]^-$ CN bond distances are much longer and range from 1.280 (12) to 1.308 (12) Å and average 1.294 Å. Furthermore, *cis*-N–Mn–N' bond angles display a distortion from 90° and range from 85.1 (2) to 92.9 (2)°. The smallest N–Mn–O(1) and N–Mn–O(2) bond angles deviate appreciably from 90° and are 78.9 (4) and 76.9 (4)°, respectively. Nonlinear coordination of the $[N(CN)_2]^-$ ligands to the Mn^{II} center is apparent with Mn–N(2)–C(2) and Mn–N(5)–C(4) bond angles of 170.2 (6) and 167.4 (7)°, respectively. Interestingly, 1-D chains akin to **2** do not form but instead unusual cylindrical tubes containing coordinated and lattice H_2O molecules are produced; see Fig. 6. O(3) and O(4) belong to the noncoordinated H_2O molecules and reside on the twofold axis along *c*. Elongated hexagonal cavities with the six vertices consisting of two Mn^{II} and four $[N(CN)_2]^-$ ligands are evident in Fig. 7. Figure 8 displays the packing arrangement of **4**. The intrachain Mn···Mn separations are 7.949 and 8.326 Å for the side sharing and cross-linking $[N(CN)_2]^-$ ligands, respectively. The chains are isolated from one another by the monodentate 4,4'-bipyridine ligands that in effect push them apart. This structure represents a rare example of a monodentate 4,4'-bipyridine ligand; others known include Ni(II) (23a) and Cu(II) (23b) complexes.

Magnetic Properties

The magnetic susceptibilities of **2**, **3**, and **4** have been measured between 2 and 300 K and can be fit by the Curie–Weiss expression, $\chi \propto (T - \theta)^{-1}$, with $g = 2.00$ and $\theta = -1.90$, -3.5, and -4.7 K, respectively, indicative of weak antiferromagnetic interactions between nearest-neighbor Mn^{II} ions. The room temperature effective moments are 5.89, 5.86, and 5.81 μ_B, respectively, and are in excellent agreement with the spin-only value of 5.92 μ_B expected for uncoupled high-spin $S = 5/2$ ions. In each material, the moment remains nearly constant to about 125 K before
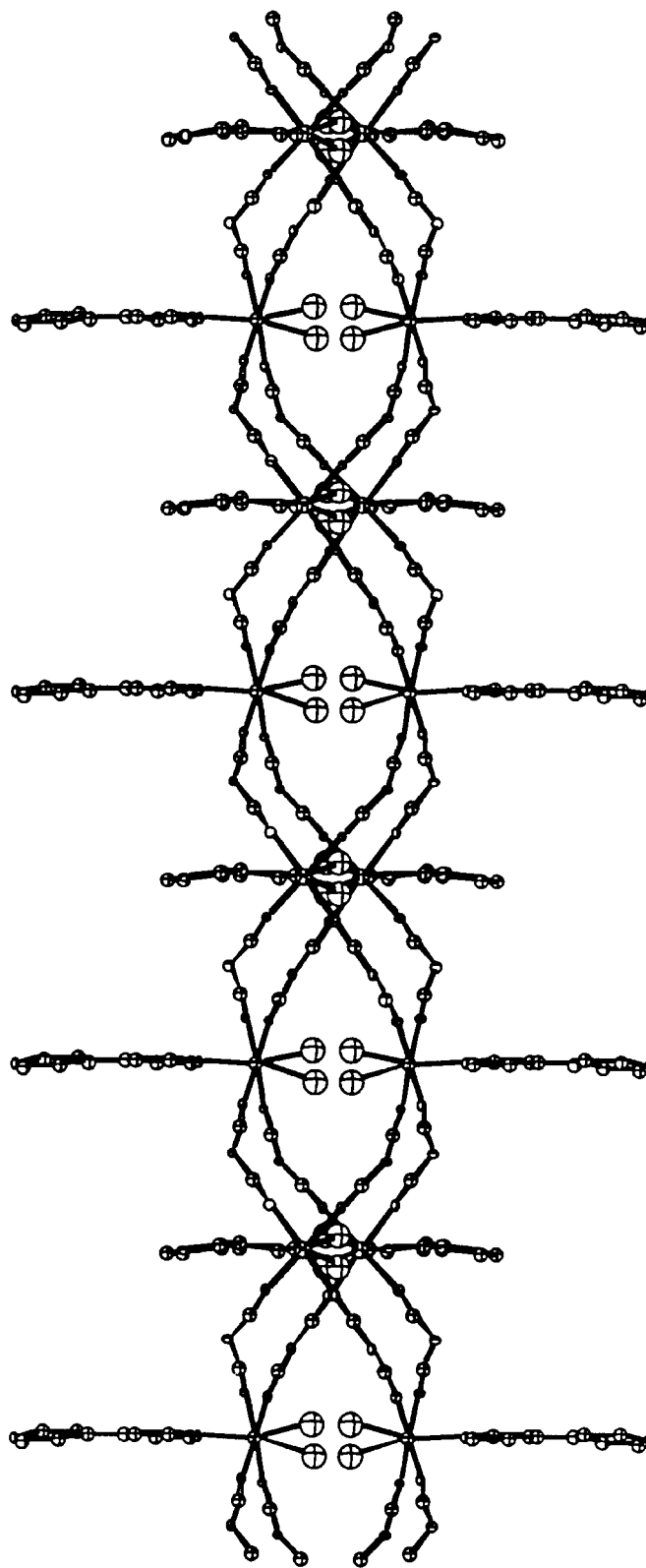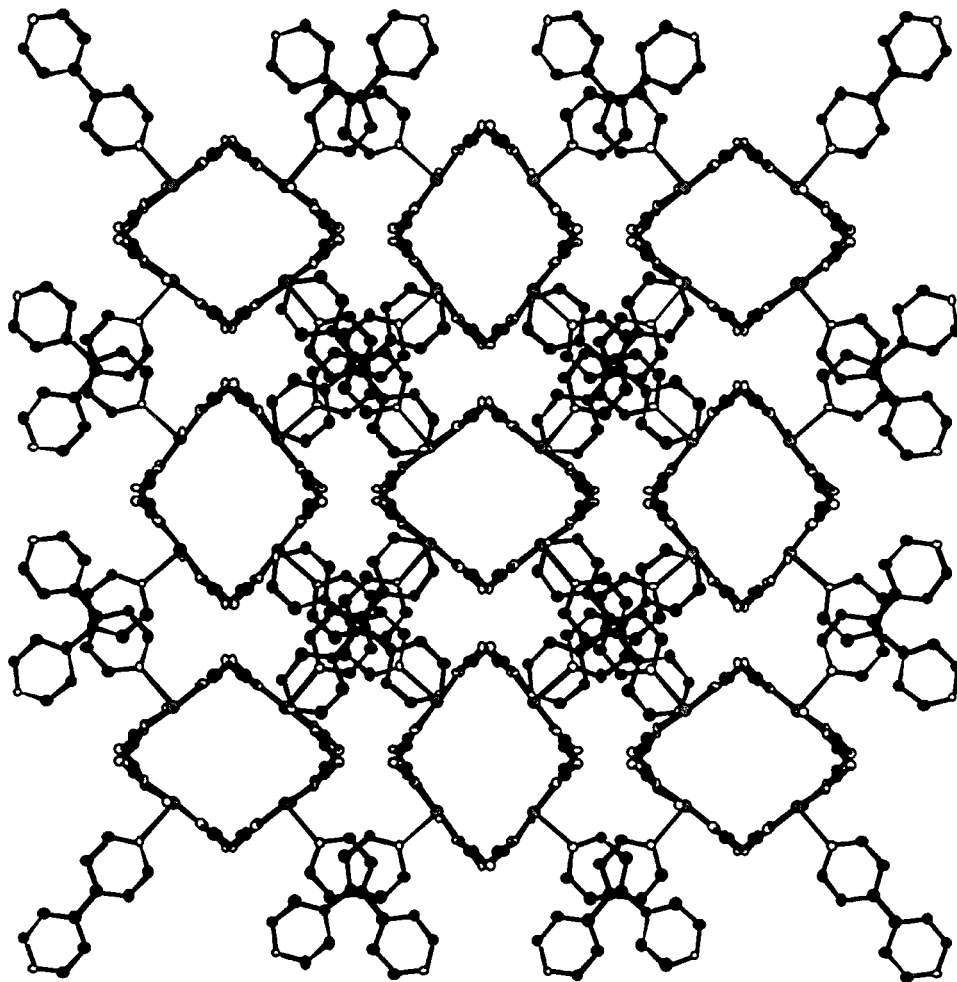

FIG. 7. View of the 1-D chain in **4** depicting the alternating hexagonal segments that are occupied by both coordinated and noncoordinated water molecules. The noncoordinated H_2O molecule has been omitted for clarity but is located near the coordinated ones.

FIG. 8. Pseudo-face-centered cubic crystal packing arrangement observed in **4** viewed down the *c*-axis. The H_2O molecules have been omitted for clarity.

decreasing abruptly below 50 K because of antiferromagnetic coupling. In order to elucidate the intrachain exchange interaction between isotropic Mn^{II} centers, χ_{dc} was also fit (2–300 K) to the Heisenberg infinite linear chain model derived by Fisher (24), (Fig. 9),

$$\chi = \frac{Ng^2\mu_B^2 S(S+1)}{3k_B T} \cdot \frac{1 + u(K)}{1 - u(K)} \qquad [1]$$

$$K = \frac{2JS(S+1)}{k_B T}, \quad u(K) = \coth K - \frac{1}{K}.$$

where N is Avogadro's number, μ_B is Bohr magneton, k_B is Boltzmann's constant, and J is the intrachain coupling constant.

Application of this approximation is valid for systems with a large number of spins, such as $S = 5/2$ Mn^{II}. The best-fit parameters of the experimental data to the theoretical model are $g = 2.00$ and $J/k_B = -0.10$, -0.17, and -0.24 K for **2**, **3**, and **4**, respectively, and signify weak isotropic antiferromagnetic intrachain interactions. Interchain interactions are expected to be negligible due to large distances between chains with the shortest $Mn \cdots Mn$ separations being 8.698, 6.677, and 7.510 Å for **2**, **3**, and **4**, respectively. Due to weak antiferromagnetic coupling propagated along the MnNCNCNM bridge, no long-range magnetic ordering was observed above 2 K, although the onset of a peak maximum in χ_{dc} is observed for **4**. The enhanced interaction of **3** relative to **2** suggests a more efficient superexchange pathway when the chains adopt a *cis*-configuration as opposed to the *trans*-configuration found in **2**.
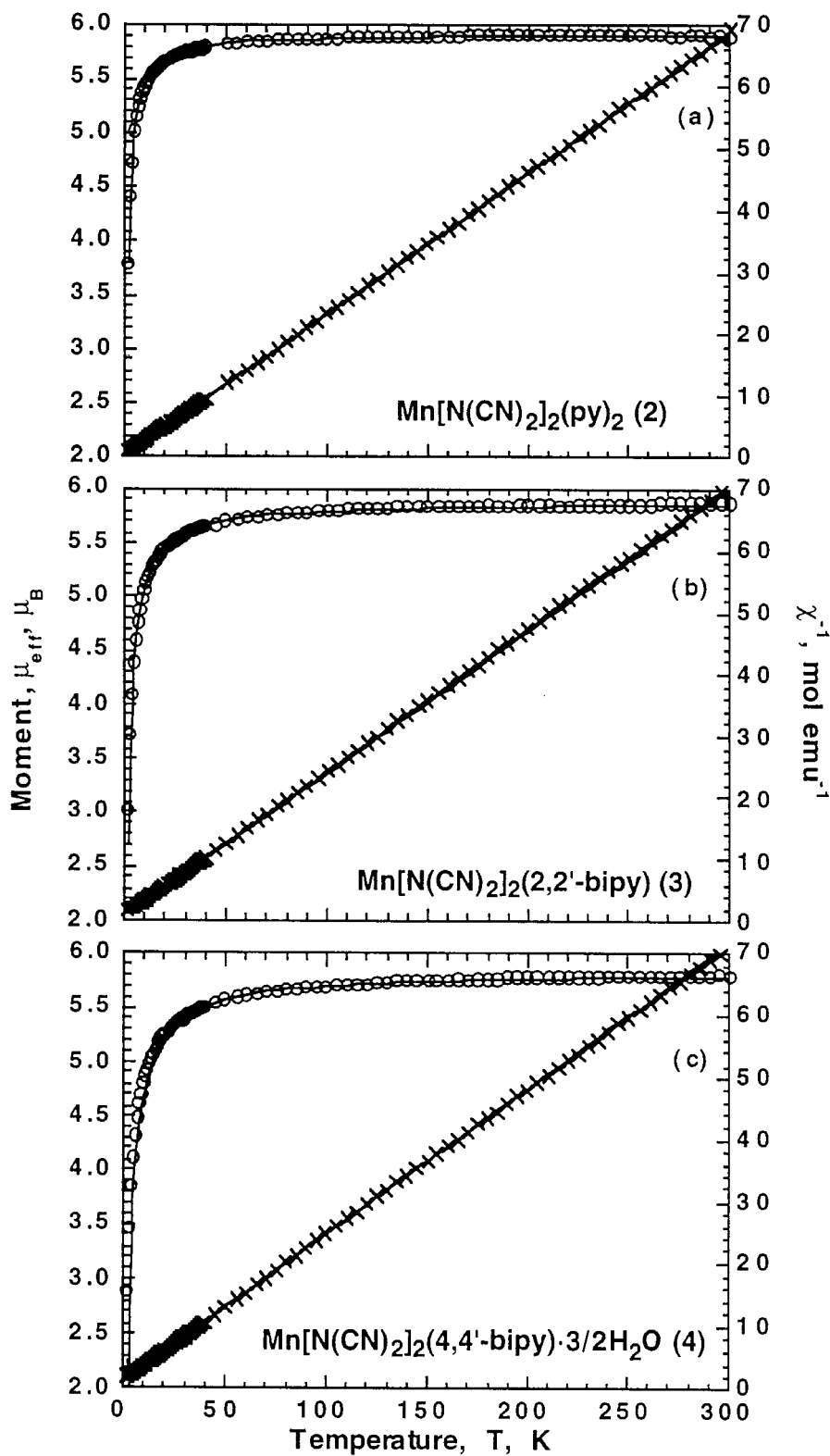
FIG. 9. Temperature dependence of the effective moment (o) and reciprocal molar magnetic susceptibility ($\times$) of **2** (a), **3**, (b), and **4** (c), The data were fitted to the expression derived by Fisher for an isotropic Heisenberg 1-D chain (—) with $S = 5/2$, $g = 2.00$, and $J/k_B = -0.10$, -0.17, and -0.24 K, for **2**, **3**, and **4**, respectively.

ACKNOWLEDGMENTS

REFERENCES

1. e.g., M. Fujita, Y. J. Kwon, S. Washizu, and K. Ogura, *J. Am. Chem. Soc.* **116,** 1151 (1994).

2. e.g., A. Aumuller, P. Erk, G. Klebe, S. Hünig, J. U. von Schütz, and H.-P. Werner, *Angew. Chem. Int. Ed. Engl.* **25,** 740 (1986).

3. e.g., B. F. Hoskins and R. Robson, *J. Am. Chem. Soc.* **112,** 1546 (1990); P. J. Stang and B. Olenyuk, *Acc. Chem. Res.* **30,** 502 (1997).

4. (a) J. S. Miller and A. J. Epstein, *Angew. Chem. Int. Ed. Engl.* **33,** 385 (1994); *Angew. Chem.* **106,** 399 (1994); (b) D. Gatteschi, *Adv. Mat.* **6,** 635 (1994); (c) J. S. Miller and A. J. Epstein, *Adv. Chem. Ser.* **245,** 161 (1995); (d) O. Kahn, "Molecular Magnetism." VCH, Weinheim/New York, 1993; (e) J. S. Miller and A. J. Epstein, *J. Chem. Soc. Chem. Commun.*, 1319 (1998).

5. (a) J. S. Miller, J. C. Calabrese, A. J. Epstein, R. W. Bigelow, J. H. Zhang, and W. M. Reiff, *J. Chem. Soc. Chem. Commun.*, 1026 (1986); (b) J. S. Miller, J. C. Calabrese, H. Rommelmann, S. R. Chittipeddi, J. H. Zhang, W. M. Reiff, and A. J. Epstein, *J. Am. Chem. Soc.* **109,** 769 (1987).

6. Y. Pei, M. Verdaguer, and O. Kahn, *J. Am. Chem. Soc.* **108,** 428 (1986).

7. J. M. Manriquez, G. T. Yee, R. S. McLean, A. J. Epstein, and J. S. Miller, *Science* **252,** 1415 (1991).

8. J. Zhang, J. Ensling, V. Ksenofontov, P. Gütlich, A. J. Epstein, and J. S. Miller, *Angew. Chem. Int. Ed.* **37,** 657 (1998).

9. (a) S. Ferlay, T. Mallah, R. Ouahes, P. Veillet, and M. Verdaguer, *Nature* **378,** 701 (1995); (b) H. Miyasaka, N. Matsumoto, H. Okawa, N. Re, E. Gallo, and C. Floriani, *Angew. Chem. Int. Ed. Engl.* **34,** 1446 (1995); (c) W. R. Entley and G. S. Girolami, *Science* **268,** 397 (1995).

10. M. Ohba, H. Okawa, T. Ito, and A. Ohto, *J. Chem. Soc. Chem. Commun.*, 1545 (1995); S. Decurtins, H. W. Schmalle, R. Pellaux, P. Schneuwly, and A. Hauser, *Inorg. Chem.* **35,** 1451 (1996); S. Decurtins, H. W. Schmalle, H. R. Oswald, A. Linden, J. Ensling, P. Gütlich, and A.

Hauser, *Inorg. Chim. Acta.* **216,** 65 (1994); R. Pellaux, H. W. Schmalle, R. Huber, P. Fischer, T. Hauss, B. Ouladdiaf, and S. Decurtins, *Inorg. Chem.* **36,** 2301 (1997).

11. e.g., (a) X. Ouyang, C. Campana, and K. R. Dunbar, *Inorg. Chem.* **35,** 7188 (1996); (b) F. A. Cotton and Y. Kim, *J. Am. Chem. Soc.* **115,** 8511 (1993); (c) F. A. Cotton, Y. Kim, and J. Lu, *Inorg. Chim. Acta.* **221,** 1 (1994); (d) C. Campana, K. R. Dunbar, and X. Ouyang, *J. Chem. Soc. Chem. Commun.* 2427 (1996).

12. Y. M. Chow and D. Britton, *Acta. Crystallogr. B* **31,** 1934 (1975).

13. I. Potocnák, M. Dunaj-Jurco, D. Miklos, and L. Jäger, *Acta. Crystallogr. C* **52,** 1653 (1996).

14. I. Potocnák, M. Dunaj-Jurco, D. Miklos, and Kabesová, *Acta. Crystallogr. C* **51,** 600 (1995).

15. (a) D. Britton and Y. M. Chow, *Acta. Crystallogr. B* **33,** 697 (1977); (b) D. Britton, *Acta. Crystallogr. C* **46,** 2297 (1990).

16. Y. M. Chow, *Inorg. Chem.* **10,** 1938 (1971).

17. J. L. Manson, D. W. Lee, A. L. Rheingold, and J. S. Miller, *Inorg. Chem.* **37,** 5966 (1998).

18. (a) J. L. Manson, C. R. Kmety, Q. Huang, J. W. Lynn, G. Bendele, S. Pagola, P. W. Stephens, L. Liable-Sands, A. L. Rheingold, A. J. Epstein, and J. S. Miller, *Chem. Mater.* **10,** 2552 (1998); (b) S. R. Batten, P. Jensen, B. Moubaraki, K. S. Murray, and R. J. Robson, *J. Chem. Soc. Chem. Commun.*, 439 (1998).

19. G. B. Kauffman, R. A. Albers, and F. L. Harlan, *Inorg. Syn.* **12,** 251 (1970).

20. G. Sheldrick, SHELX-v5.0, Program for Crystal Structure Determination. Bruker, Madison, WI.

21. A. Altomare, M. C. Burla, M. Camalli, G. Cascarano, C. Giacovazzo, A. Guagliardi, A. G. G. Moliterni, G. Polidori, and R. Spagna, submitted for publication.

22. (a) J. L. Manson, C. Campana, and J. S. Miller, *J. Chem. Soc. Chem. Commun.*, 251 (1998); (b) K. Fegy, D. Luneau, T. Ohm, C. Paulsen, and P. Rey, *Angew. Chem. Int. Ed. Engl.* **37,** 1270 (1998); (c) J. Larionova, J. Sanchiz, S. Gohlen, L. Ouahab, and O. Kahn, *J. Chem. Soc. Chem. Commun.* 953 (1998); (d) M.-X. Li, G.-Y. Xie, Y.-D. Gu, J. Chen, and P.-J. Zheng, *Polyhedron.* **14,** 1235 (1995).

23. (a) O. M. Yaghi, H. Li, and T. L. Groy, *Inorg. Chem.* **36,** 4292 (1997); (b) M. Julve, M. Verdaguer, J. Faus, F. Tinti, J. Moratal, A. Monge, and E. Gutierrez-Publa, *Inorg. Chem.* **26,** 3520 (1987).

24. M. E. Fisher, *Am. J. Phys.* **32,** 343 (1964).